AGU PUBLICATIONS

JGR

Journal of Geophysical Research: Atmospheres

RESEARCH ARTICLE
10.1002/2017JD027703

Key Points:
- The ensemble of 13 RCMs accurately reproduces the spatial distribution of cyclone characteristics in the Arctic, compared to four reanalyses
- The variations of cyclone frequency across the ensemble are largest for small (radius up to 400 km) and shallow cyclones (depth up to 4 hPa)
- Nudged RCMs represent cyclone characteristics and trends more accurately due to realistic representation of zonal winds and temperature

Supporting Information:
- Supporting Information S1

Correspondence to:
M. Akperov,
aseid@ifaran.ru

Citation:
Akperov, M., Rinke, A., Mokhov, I. I., Matthes, H., Semenov, V. A., Adakudlu, M., et al. (2018). Cyclone activity in the Arctic from an ensemble of regional climate models (Arctic CORDEX). *Journal of Geophysical Research: Atmospheres*, *123*, 2537–2554. https://doi.org/10.1002/2017JD027703

Received 6 SEP 2017
Accepted 3 FEB 2018
Accepted article online 10 FEB 2018
Published online 7 MAR 2018
Corrected 25 MAY 2018

This article was corrected on 25 MAY 2018. See the end of the full text for details.

Cyclone Activity in the Arctic From an Ensemble of Regional Climate Models (Arctic CORDEX)

Mirseid Akperov[1], Annette Rinke[2], Igor I. Mokhov[1,3], Heidrun Matthes[2], Vladimir A. Semenov[1,4], Muralidhar Adakudlu[5], John Cassano[6], Jens H. Christensen[5,7], Mariya A. Dembitskaya[1], Klaus Dethloff[2], Xavier Fettweis[8], Justin Glisan[9], Oliver Gutjahr[10], Günther Heinemann[11], Torben Koenigk[12,13], Nikolay V. Koldunov[14,15], René Laprise[16], Ruth Mottram[17], Oumarou Nikiéma[16], John F. Scinocca[18], Dmitry Sein[14,19], Stefan Sobolowski[5], Katja Winger[16], and Wenxin Zhang[20,21]

[1]A.M. Obukhov Institute of Atmospheric Physics, RAS, Moscow, Russia, [2]Alfred Wegener Institute, Helmholtz Centre for Polar and Marine Research, Potsdam, Germany, [3]Department of Physics, Lomonosov Moscow State University, Moscow, Russia, [4]Institute of Geography, RAS, Moscow, Russia, [5]Uni Research Climate, Bjerknes Centre for Climate Research, Bergen, Norway, [6]Cooperative Institute for Research in Environmental Sciences and Department of Atmospheric and Oceanic Sciences, University of Colorado Boulder, Boulder, CO, USA, [7]Niels Bohr Institute, University of Copenhagen, Copenhagen, Denmark, [8]Department of Geography, University of Liège, Liege, Belgium, [9]Department of Geological and Atmospheric Sciences, Iowa State University, Ames, IA, USA, [10]Max Planck Institute for Meteorology, Hamburg, Germany, [11]Environmental Meteorology, Faculty of Regional and Environmental Sciences, University of Trier, Trier, Germany, [12]Rossby Centre, Swedish Meteorological and Hydrological Institute, Norrköping, Sweden, [13]Department of Meteorology, Bert Bolin Centre for Climate Research, Stockholm University, Stockholm, Sweden, [14]Alfred Wegener Institute, Helmholtz Centre for Polar and Marine Research, Bremerhaven, Germany, [15]MARUM - Center for Marine Environmental Sciences, Bremen, Germany, [16]Centre ESCER, Université du Québec à Montréal, Montréal, Québec, Canada, [17]Danish Meteorological Institute, Copenhagen, Denmark, [18]Canadian Centre for Climate Modelling and Analysis, Environment and Climate Change Canada, Victoria, British Columbia, Canada, [19]Shirshov Institute of Oceanology, RAS, Moscow, Russia, [20]Department of Physical Geography and Ecosystem Science, Lund University, Lund, Sweden, [21]Center for Permafrost, Department of Geosciences and Natural Resource Management, University of Copenhagen, Copenhagen, Denmark

Abstract The ability of state-of-the-art regional climate models to simulate cyclone activity in the Arctic is assessed based on an ensemble of 13 simulations from 11 models from the Arctic-CORDEX initiative. Some models employ large-scale spectral nudging techniques. Cyclone characteristics simulated by the ensemble are compared with the results forced by four reanalyses (ERA-Interim, National Centers for Environmental Prediction-Climate Forecast System Reanalysis, National Aeronautics and Space Administration-Modern-Era Retrospective analysis for Research and Applications Version 2, and Japan Meteorological Agency-Japanese 55-year reanalysis) in winter and summer for 1981–2010 period. In addition, we compare cyclone statistics between ERA-Interim and the Arctic System Reanalysis reanalyses for 2000–2010. Biases in cyclone frequency, intensity, and size over the Arctic are also quantified. Variations in cyclone frequency across the models are partly attributed to the differences in cyclone frequency over land. The variations across the models are largest for small and shallow cyclones for both seasons. A connection between biases in the zonal wind at 200 hPa and cyclone characteristics is found for both seasons. Most models underestimate zonal wind speed in both seasons, which likely leads to underestimation of cyclone mean depth and deep cyclone frequency in the Arctic. In general, the regional climate models are able to represent the spatial distribution of cyclone characteristics in the Arctic but models that employ large-scale spectral nudging show a better agreement with ERA-Interim reanalysis than the rest of the models. Trends also exhibit the benefits of nudging. Models with spectral nudging are able to reproduce the cyclone trends, whereas most of the nonnudged models fail to do so. However, the cyclone characteristics and trends are sensitive to the choice of nudged variables.

1. Introduction

Cyclones contribute to the meridional atmospheric heat and moisture transport from midlatitudes into the Arctic, thereby changing cloud feedback with impacts on the sea-ice retreat in a warming climate (Chernokulsky et al., 2017; Mokhov et al., 2009; Simmonds & Keay, 2009; Zhang et al., 2013). Advection of heat by eddies from lower latitudes provides more than half of the annual heat transport to the Arctic climate system and most of the heat transport in winter. Sea-ice changes can impact the cyclone activity in the Arctic by

modifying the baroclinicity (e.g., Inoue et al., 2012; Rinke et al., 2013), and in turn, cyclones can affect the sea ice. An example of the latter was the destruction of sea ice by the intense Arctic cyclone that occurred in summer 2012 contributing to the record sea-ice minimum that year (Kriegsmann & Brümmer, 2014; Parkinson & Comiso, 2013; Simmonds & Rudeva, 2012; Zhang et al., 2013). Thus, cyclones are a key component of the Arctic climate system and their representation in climate models should therefore be realistic.

Long-term changes in cyclone activity over the Arctic have been analyzed in many studies based on reanalysis data (Brümmer et al., 2000; Koyama et al., 2017; McCabe et al., 2001; Sepp & Jaagus, 2011; Simmonds et al., 2008; Zhang et al., 2004). Using National Centers for Environmental Prediction (NCEP)/National Center for Atmospheric Research reanalysis, Sepp & Jaagus (2011) found an increasing number of cyclones (including deep cyclones) in the Arctic in winter and summer in the last decades. Using the same data and period, Zhang et al. (2004) noted that the number and intensity of cyclones entering the Arctic from the midlatitudes have increased, particularly in summer. The same results were obtained by McCabe et al. (2001) for winter but for the last four decades. Akperov and Mokhov (2013) found an increase in the number and a decrease in the mean size of cyclones in the polar regions (north of 60°N) using NCEP/National Center for Atmospheric Research reanalysis data for the 1948–2007 period. However, Simmonds et al. (2008) showed that different cyclone characteristic trends depend on both the analyzed period and the choice of reanalysis data.

Simmonds et al. (2008) noted a link between the Arctic Oscillation (AO) phase and cyclone characteristics, wherein a positive phase of the AO is associated with more frequent, deeper, and larger cyclonic systems in the Arctic region. The correlations with AO are particularly strong in summer as discussed by Serreze and Barrett (2008). Variability in extreme cyclones is closely linked with the winter AO (Thompson & Wallace, 1998). This suggests that a positive AO index is associated with an increase of baroclinicity, increasing cyclogenesis, and number of extreme cyclones in the Arctic.

Cyclone activity in the Arctic under current and future climate has been investigated in global climate models (GCMs) (e.g., Christensen et al., 2013; Nishii et al., 2015; Orsolini & Sorteberg, 2009; Vavrus, 2013). Vavrus (2013) showed that Coupled Model Intercomparison Project Phase 5 (CMIP5) models are able to reproduce the basic characteristics of extreme Arctic cyclones in the Arctic, despite their relatively coarse resolution. However, the low resolution of these models generally prevents the appropriate representation of mesoscale polar lows (diameter ~400 km).

An alternative approach to analyze cyclone activity over the Arctic is regional climate models (RCMs) and, in particular, ensembles of RCMs. This approach combines the benefits of a multimodel ensemble with the increased resolution to provide a platform for a robust analysis of Arctic cyclone activity. The Arctic CORDEX initiative (COordinated Regional climate Downscaling EXperiment; http://climate-cryosphere.org/activities/targeted/polar-cordex/arctic) is an international coordinated framework to produce an improved ensemble of regional climate change projections as the input for impact and adaptation studies aimed at a better understanding of the regional climate in the Arctic. Unlike GCMs, RCMs can adequately resolve mesoscale processes that are crucial for representing the mesoscale cyclones, in particular polar lows (Akperov et al., 2015; Shkolnik & Efimov, 2013; Spengler et al., 2017).

One way of improving atmospheric circulation and cyclone activity in RCMs is the application of a spectral nudging (SN) procedure (von Storch et al., 2000). SN is a method whereby the large spatial scales of the RCM are nudged toward the large scales of the driving reanalysis in order to achieve an atmospheric state in the regional domain close to the driving field. As noted by Berg et al. (2013) the SN reduces biases throughout the free troposphere and improves the mean sea level pressure (MSLP). Previous studies have shown that RCMs with the use of SN successfully reproduce polar low characteristics in the Arctic (Kolstad & Bracegirdle, 2016; Zahn & Von Storch, 2008). RCMs with SN also show a good representation of extratropical cyclone characteristics (Côté et al., 2015).

Based on CMIP3/5 models' analysis, Nishii et al. (2015) showed that the spatial patterns of cyclone activity over the Arctic in summer are closely connected with climatological circulation fields. A close association of the cyclone activity with the mean zonal wind at 250 hPa was found in the Norwegian Sea area in winter and summer for CMIP5 models (Seiler & Zwiers, 2016; Zappa et al., 2013). Orsolini and Sorteberg (2009) noted that changes in high-latitude 300 hPa zonal winds and storminess are connected with the increase in the surface thermal contrast between the Eurasian continent and the Arctic Ocean in summer. Woollings et al. (2010)

found a linkage between the cyclone track density and 250 hPa zonal wind biases in the North Atlantic. Mizuta (2012) noted a relationship between the number of intense cyclones and jet stream speed over the North Pacific. However, over the North Atlantic, they only found a weak association, which is possibly related to a disagreement in surface temperature change in models affected by the circulation changes in the Atlantic Ocean. Therefore, it is interesting to examine the impact of different nudging methods in RCMs on the representation of atmospheric circulation and their connection with cyclone activity in the Arctic.

The aim of this study is to assess the performance of Arctic CORDEX RCMs relative to several reanalysis products and to evaluate the role of large-scale SN in representing cyclone activity characteristics and their spatio-temporal variability. Understanding the physical mechanisms beyond intermodel spread and biases in cyclone activity characteristics in current climate may help to improve the simulation Arctic processes by climate models.

2. Data and Methods

2.1. Model and Reanalysis Data

We analyze cyclone characteristics obtained from 6-hourly MSLP data from an ensemble of 13 atmospheric RCM simulations and four reanalysis products (Table 1) during the 1981–2010 period for the Arctic region (north of 65°N) for two seasons—winter (December-January-February) and summer (June-July-August). COSMO Climate Limited-area Model (CCLM) data are only available for the winter season. We also analyze monthly mean zonal wind at 850 and 200 hPa for both seasons.

The five reanalysis products used are ERA-Interim, NCEP-Climate Forecast System Reanalysis (CFSR), National Aeronautics and Space Administration-Modern-Era Retrospective analysis for Research and Applications Version 2 (NASA-MERRA2), Japan Meteorological Agency-Japanese 55-year reanalysis (JMA-JRA55), and Arctic System Reanalysis version 2 (ASRv2), hereafter called ERA-Interim, CFSR, MERRA2, JRA55, and ASR (Table 1). The reanalysis data sets vary from 15 to 75 km in the horizontal resolution and from 60 to 72 levels in the vertical resolution. ASR data cover only short period (2000–2010), and all comparison of ASR to ERA-linterim or other reanalyses is based on this shorter period (if not otherwise noted).

The 13 Arctic CORDEX RCM simulations (Table 1) are based on the standard Arctic CORDEX model setup (http://climate-cryosphere.org/activities/targeted/polar-cordex/arctic). The domain and the horizontal resolution are nearly the same (0.44° or ~45 km). Only the CCLM model applies a higher resolution (15 km), but data are only available for the winter season. The vertical resolution and domain extent varies from model to model, from 23 to 60 levels. The models use the same lateral atmospheric boundary conditions from the ERA-Interim data and over ocean; sea surface temperature and sea-ice concentration are also obtained from ERA-Interim. An exception is the CCLM model where satellite-derived sea-ice concentration (European Organisation for the Exploitation of Meteorological Satellites, 2015) and ice thickness from Pan-Arctic Ice Ocean Modeling and Assimilation System (PIOMAS) (Zhang & Rothrock, 2003) are used. Some of the models use large-scale SN, some run free (without nudging). One of the models (RCM RCA4 coupled with dynamic vegetation and ecosystem biogeochemistry simulated by the vegetation-ecosystem model LPJ-GUESS (RCA-GUESS)) has the Land Surface Scheme coupled with dynamic vegetation and ecosystem biogeochemistry simulated by the vegetation-ecosystem model Lund-Potsdam-Jena General Ecosystem Simulator (Smith et al., 2011; Zhang et al., 2014). More detailed information about the RCMs (resolution, nudged fields, etc.) is presented in Table 1. All reanalysis and model data adopt the Arctic CORDEX grid (rotated 0.44° × 0.44° grid, 116 × 133 grid points).

2.2. Cyclone Identification

We use an algorithm of cyclone identification similar to Bardin and Polonsky (2005) and Akperov et al. (2007) with some modifications for the Arctic region (Akperov et al., 2015). The algorithm is based on the MSLP field and has been shown to be useful to investigate the changes in cyclone activity in extratropical and high latitudes (Akperov et al., 2015; Akperov & Mokhov, 2010; Neu et al., 2013; Simmonds & Rudeva, 2014; Ulbrich et al., 2013). It should be noted that more than half of the cyclone identification methods presented in the Intercomparison of Mid Latitude Storm Diagnostics project (Neu et al., 2013) are pressure-based identification methods. MSLP fields are also used to detect intense polar mesocyclones (polar lows) in the Arctic that form during the cold season over the relatively warm open water in the Arctic (Rasmussen & Turner, 2003). Cyclones can also be detected based on vorticity maps. However, the vorticity-based method strongly

Table 1
Reanalysis and Arctic CORDEX Models and Their Corresponding Information

Type	Institution/ country	Data/model name	Original resolution vertical, horizontal	Nudging	Sea-ice thickness	Reference
Reanalyses	ECMWF/UK	ERA-Interim	L60, 0.75° (~75 km)			Dee et al. (2011)
	NASA/USA	MERRA2	L72, 0.5° × 0. 625° (~50 km)			Gelaro et al. (2017)
	NCEP/USA	CFSR	L64, 0.5° (~50 km)			Saha et al. (2010)
	JMA/JAPAN	JRA55	L60, 0.5° (~50 km)			Ebita et al. (2011); Kobayashi et al. (2015);
	PMG/ASR	ASR	L71, 15 km (~0.12°)			Bromwich et al. (2017)
Regional Climate Models (RCMs)	CCLM/Germany	CCLM	L60, 0.125° (~15 km)	***w/o***	PIOMAS climatology	Gutjahr et al. (2016)
	CCCma/Canada	CanRCM4	L32, 0.44° (~45 km)	Spectral (***U***, ***V***, above 850 hPa)	Spatially varying monthly climatology	Scinocca et al. (2016)
	GERICS/Germany	REMO	L40, 0.5° (~50 km)	***w/o***	2 m	Sein et al. (2014, 2015)
	AWI/Germany	HIRHAM5-AWI	L40, 0.5° (~50 km)	Grid point (***T***, ***U***, ***V***, ***Q***)	2 m	Christensen et al. (2007); Sommerfeld et al. (2015); Klaus et al. (2016)
	DMI/Denmark	HIRHAM5-dmi	L31, 0.44° (~45 km)	***w/o***	2 m	Christensen et al. (2007); Lucas-Picher et al. (2012)
	SMHI/Sweden	RCA4 RCASN	L40, 0.44°, (~45 km)	***w/o*** Spectral (***U***, ***V***, ***T,*** above 850 hPa)	1 m	Berg et al. (2013); Koenigk et al. (2015)
	LU/Sweden	RCA-GUESS	L40, 0.44°, (~45 km)	***w/o***	1 m	Smith et al. (2011); Zhang et al. (2014)
	MGO/Russia	RRCM	L25, 50 km (~0.5°)	***w/o***	1.5 m	Shkolnik and Efimov (2013)
	ULg/Belgium	MAR3.6	L23, 50 km (~0.5°)	Spectral (***U***, ***V***, ***T*** for lower stratosphere)	0.5 m	Fettweis et al. (2017)
	UNI/Norway	WRF3.3.1	L51, 0.44°, (~45 km)	***w/o***	3 m	Skamarock et al. (2008)
	UQAM/Canada	CRCM5 CRCMSN	L55, 0.44°, (~45 km)	***w/o*** Spectral (***U***, ***V,*** above 850 hPa)	0.001–2.5 m	Martynov et al. (2013); Šeparović et al. (2013); Takhsha et al. (2017)

Note. ***U***, zonal wind; ***V***, meridional wind; ***T***, temperature; ***Q***, humidity; ***w/o***, without nudging.

depends on the spatial resolution of the data and produces more small-scale cyclones than the pressure-based method. In case of polar lows, Laffineur et al. (2014) cautioned to use a vorticity-based method for polar low identification and tracking because vorticity maxima can also be associated with troughs. Hence, we choose cyclone characteristics using MSLP data fields.

We calculate cyclone frequency, depth, and size. The cyclone frequency is defined as the number of cyclone events per season. To map spatial patterns of cyclone characteristics, we use the grid with circular cells of a 2.5° latitude radius. The temporal and spatial correlation analysis is based upon the Pearson correlation coefficient (R). As an indicator of the robustness of any trends we calculate their statistical significance using a Student's t test at the 90% confidence level ($P < 0.1$).

We consider depth as a measure of cyclone intensity. The cyclone depth is determined as a difference between the minimum central pressure in the cyclone and the outermost closed isobar. As shown in previous studies (Golitsyn et al., 2007; Simmonds & Keay, 2009), the depth provides a direct measure of the kinetic energy of the system. Deep cyclones are identified by anomalously strong depth exceeding an arbitrary threshold chosen to be the 95th percentile of cyclone depth distribution from ERA-Interim reanalyses, which corresponds to 20 hPa. The cyclone size (radius) is determined as the average distance from the geometric center to the outermost closed isobar.

To select robust cyclone systems in the Arctic we excluded cyclones with a size less than 200 km or a depth less than 2 hPa. All cyclones over regions with surface elevations higher than 1,000 m are also excluded from the analysis due to larger uncertainty in the MSLP fields resulted from the extrapolation to the sea level. The details of this algorithm and its application for detection of the variability and changes in cyclone activity over the Arctic are discussed in previous study (Akperov et al., 2015).

3. Results

3.1. Spatial and Seasonal Cyclone Characteristics

3.1.1. Cyclone Frequency

Figure 1 displays the climatology of cyclone frequency for winter and summer from multireanalysis and the multimodel means for the period 1981–2010. The multimodel mean realistically reproduces the spatial pattern of cyclone frequency in the Arctic as compared to multireanalysis data for both seasons. In winter, maxima of

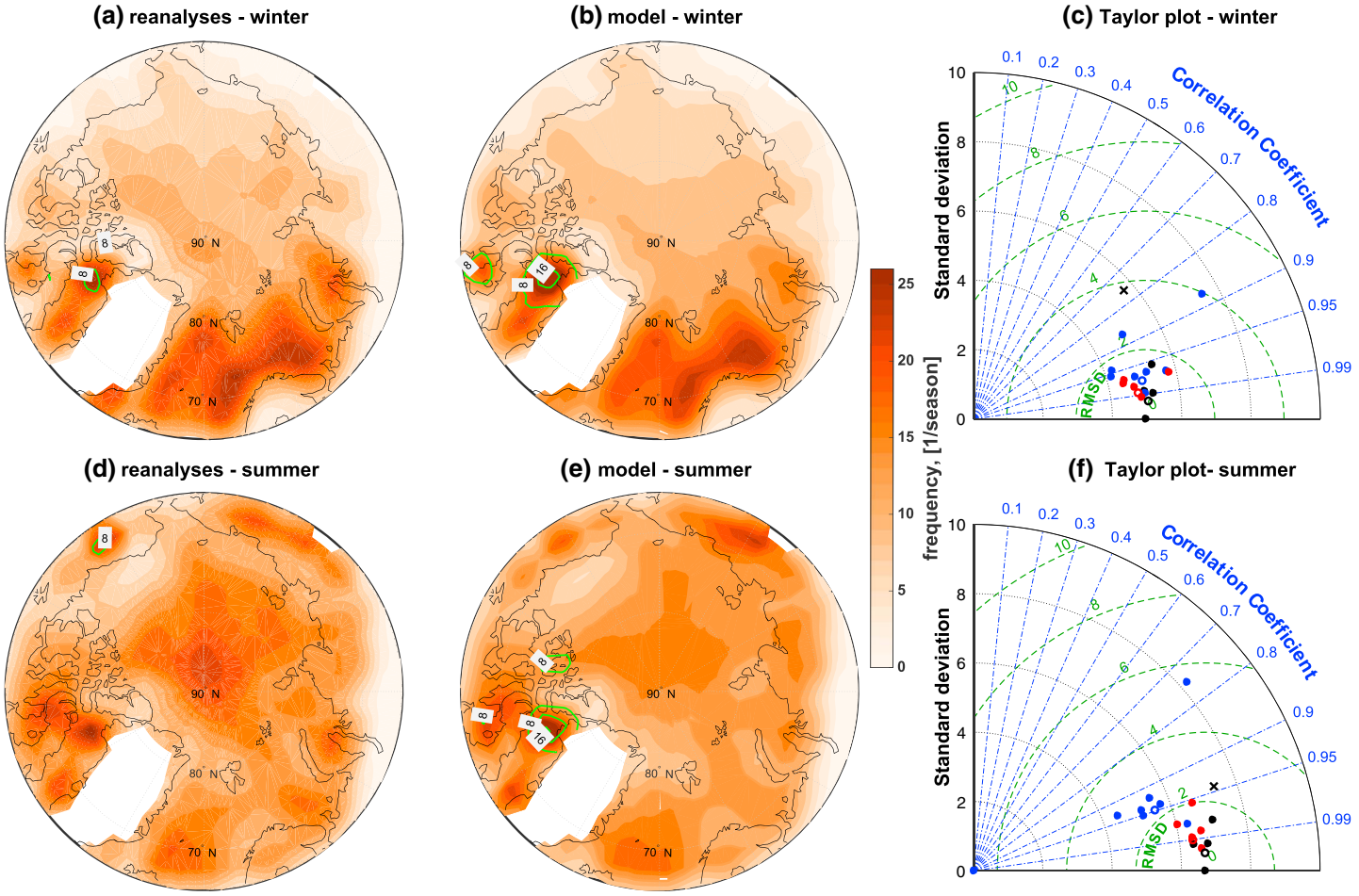

Figure 1. Spatial distribution of cyclone frequency in (a and b) winter and (d and e) summer from multireanalysis and multimodel ensemble. The green isolines indicate the standard deviations across the models or reanalyses. Taylor plots of cyclone frequency of models and reanalysis data for (c) winter and (f) summer (black dots, reanalyses; asterisk, ASR reanalysis; red dots, nudged models; blue dots, nonnudged models; black circle, multireanalysis mean; red circle, nudged multimodel ensemble mean; blue circle, nonnudged multimodel ensemble mean). Reference for Taylor plot is ERA-Interim (ref.).

cyclone frequency occur over Baffin Bay, Davis Strait, southeast of Greenland, and over the Nordic Seas. Compared to winter, the cyclone frequency in summer is lower over the region between Greenland and Barents Sea and higher over the land, in particular over Eastern Siberia, Chukotka, and Alaska and over the central Arctic. These seasonal characteristics have been discussed in previous studies (e.g., Crawford & Serreze, 2016; Simmonds et al., 2008; Wernli & Schwierz, 2006). The strongest intramodel variations in cyclone frequency are found over the Baffin Bay, Foxe Basin, and over Eastern Siberia in winter and additionally over the Queen Elizabeth Islands, and Alaska in summer.

The spatial Pearson correlation coefficients (*R*) between the individual models and ERA-Interim cyclone frequency ranges from 0.87 (Weather Research and Forecasting version 3.3.1 [WRF3.3.1]) to 0.98 (CCLM) for unnudged models and 0.97 (Canadian Centre for Climate Modelling and Analysis Regional Climate Model version 4 [CanRCM4]) to 0.99 (Alfred Wegener Institute (AWI) RCM HIRHAM version 5 (HIRHAM5-AWI)) for nudged models for winter. For summer, *R* vary from 0.75 (Voeikov Main Geophysical Observatory RCM (RRCM)) to 0.98 (Canadian Regional Climate Model [CRCM5]) for unnudged models and from 0.97 (CanRCM4) to 0.99 (HIRHAM5-AWI) for nudged models (Figures 1c and 1f). The spatial standard deviations (*SDs*) for both types of models lie in the range from 4.1 to 5.8 (cyclones per season) in winter and from 4.4 to 6.7 in summer, except for RRCM. Respective root-mean-square errors (RMSEs) vary from 0.6 to 2.5 (cyclones per season) for winter and from 0.7 to 5.4 for summer. The spatial correlation coefficients for multimodel mean for nudged/unnudged models with respect to ERA-Interim for winter and summer are 0.99/0.97 and 0.99/0.95, with *SDs* of 4.8/5.0 and 6.4/5.5 (cyclones per season), and RMSEs of 0.8/1.1 and 0.9/2.3 (cyclones per season), respectively.

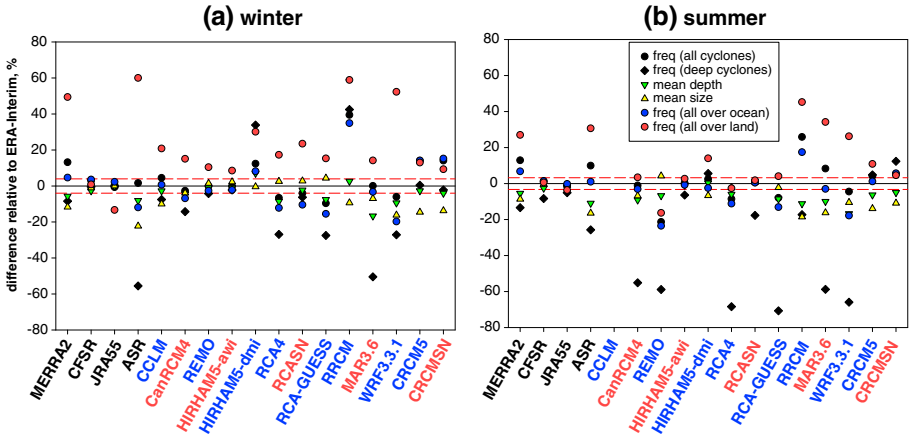

Figure 2. Relative biases of cyclone characteristics (relative to ERA-Interim), (black dot, cyclones frequency; black rhombus, deep cyclones frequency; green triangle, cyclone mean depth; yellow triangle, cyclone mean size; blue circle, cyclones frequency over oceans; red circle, cyclones frequency over land; horizontal dashed red lines, 95% confidence levels for the total cyclone frequency from ERA-Interim) in (a) winter and (b) summer. The names of the different data sets on the *x* axis are highlighted by color (black, reanalysis model, red, nudged models, blue, nonnudged models).

Most unnudged and three out of five nudged models show a lower cyclone frequency (relative to ERA-Interim) for the Arctic by up to 10% (RCA-GUESS) in winter (Figure 2). In summer, five models (of which one is nudged) show this underestimation as well, and most models (including the nudged ones) show less frequent occurrence of deep cyclones in both seasons. The underestimation ranges from 2% (RCM CRCM5 with spectral nudging (CRCMSN)) to 50% (RCM MAR version 3.6 (MAR3.6)) in winter and is up to 60% (MAR3.6) in summer for nudged models. For unnudged models, this ranges from 4% (RCM REMO (REgional MOdel) (REMO)) to 27% (RCA-GUESS) in winter and is up to 70% (RCA-GUESS) in summer. The differences between reanalyses for cyclone frequency are much smaller compared to the across-model differences. For the full overlapping period, it should be noted that the highest cyclone frequency (with respect to ERA-Interim) is found in MERRA2 in both seasons, and it is associated with shallow cyclones (e.g., Wang et al., 2016).

The frequency of cyclones over land is overestimated by all models in both seasons when compared to ERA-Interim but with a large across-model variations. This overestimation varies from 9% (HIRHAM5-AWI) to 23% (RCM RCA4 with spectral nudging (RCASN)) for the nudged and from 10% (REMO) to 59% (RRCM) for the unnudged models in winter. In summer, it varies from 2% (RCASN) to 34% (MAR3.6) and from 4% (RCA-GUESS) to 45% (RRCM), respectively. In contrast, most models underestimate the cyclone frequency over oceans in both seasons. This can reach up to 20% (WRF3.3.1) in winter and 23% (REMO) in summer. For nudged models, the variance is small and reaches up to 10% (RCASN) in winter and 3% in summer. Hence, variations in cyclone frequency across the models are partly related to the high variability in cyclone frequency over land.

The seasonal cycle is well captured by all models with high cyclone frequency in summer and low frequency in winter for all cyclones and a reverse seasonal cycle for deep cyclones (Figure 3). At the same time, models with nudging show less intraensemble variability of monthly mean cyclone frequency values compared to unnudged models. Figure 3 further shows that the spread across the models in cyclone frequency is similarly high in all months for the unnudged models than for the nudged ones.

3.1.2. Cyclone Depth and Size

The multimodel mean reproduces the spatial pattern of cyclone mean depth and size reasonably well when compared to the results from multireanalysis data for both seasons (Figure 4). In winter, the deepest cyclones are located in the region between Greenland and the Barents Sea. In summer, they shift toward the central Arctic Ocean. Cyclones with largest radii are located over the central Arctic Ocean during both seasons. This agrees with previous findings for the climatological mean depth and size for the Arctic region using different reanalysis (ERA-40 and NCEP-CFSR) and RCM data of RRCM (Akperov et al., 2015; Shkolnik & Efimov, 2013; Simmonds et al., 2008).

All individual models show good spatial correlation of cyclone mean depth in the Arctic for both seasons in comparison with ERA-Interim; the correlation coefficients vary from 0.97 (MAR3.6)/0.96 (WRF3.3.1) to 0.99 (RCASN)/0.99 (CCLM) in winter and from 0.97 (MAR3.6)/0.96 (RRCM) to 0.99 (HIRHAM5-AWI)/0.99 (CRCM5) in

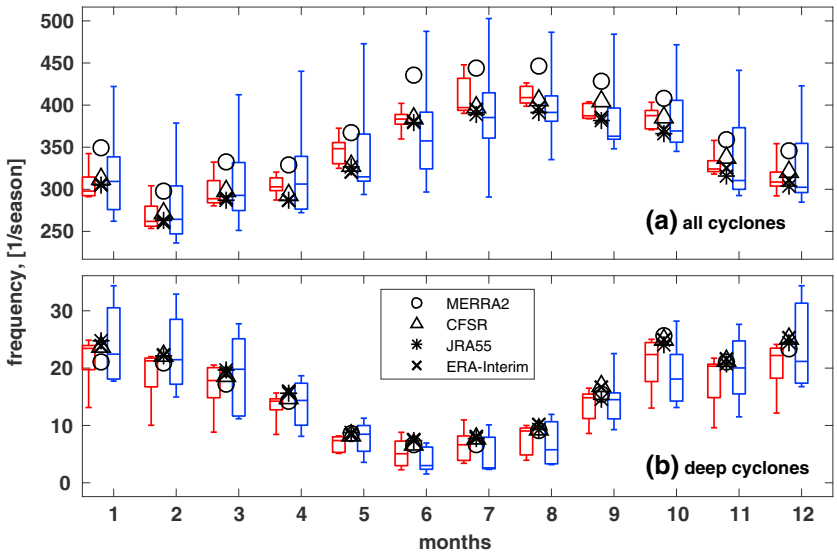

Figure 3. Annual cycle of cyclone frequency for (a) all and (b) deep cyclones from multireanalysis data and the multimodel ensemble (nudged [red] and nonnudged [blue]). The latter is given in box-whisker format and shows the minimum and maximum values, the lower and upper quartiles, and the median.

summer for the nudged/unnudged models, respectively (Figures 4c and 4f). The spatial correlation coefficients of cyclone mean depth for the nudged models are higher compared to the unnudged models. The corresponding RMSEs and *SD*s are much smaller compared to cyclone frequency statistics. Standard deviations are between 3.3/3.8 (2.9/2.8) hPa and 4.1/4.4 (3.4/3.3) hPa for winter (summer) for nudged/unnudged models while RMSEs are quite low for most of the models. The multimodel mean for nudged models outperforms that from the unnudged models for both seasons and is close to the multireanalysis mean.

Most Arctic CORDEX models show smaller cyclone mean depth when compared with ERA-Interim for both seasons (Figure 2). This underestimation varies from 1% (HIRHAM5-AWI) to 4% (CRCMSN) for the nudged models in winter with MAR3.6 being an outlier (17%). In summer, four out of five nudged models underestimate cyclone mean depth that varies from 1% (HIRHAM5-AWI) to 10% (MAR3.6). Six out of eight unnudged models show a smaller cyclone mean depth of up to 9% (WRF3.3.1) in winter. In summer, six models show a smaller mean depth and this underestimation varies from 6% (RCA4) to 17% (WRF3.3.1).

The spatial correlation for cyclone mean size between Arctic CORDEX model simulations and ERA-Interim is also high (larger than 0.98/0.96 for nudged/unnudged models) (Figures 4i and 4l). The RMSEs vary from 31/34 (12/21) km to 52/72 (61/75) km, and *SD*s vary from 207/204 (211/211) km to 246/247 (263/265) km for winter (summer) for nudged/unnudged models. The spatial correlation coefficients for the multimodel mean for summer are slightly higher for both type of models than the coefficients for winter, with R = 0.99/0.97 (0.99/0.98) with SD = 227/228 (241/240) km and RMSE = 39/58 (21/46) km for winter (summer) for nudged/unnudged models.

Most models consistently simulate smaller cyclones compared to ERA-Interim (Figure 2). Three out of five nudged models show a smaller mean size by up to 13% (CRCMSN) in winter and by up to 10% (MAR3.6) in summer. Five out of eight unnudged models underestimate cyclone mean size by up to 16% (WRF3.3.1) for winter. In summer, six models show too small cyclone mean size, which varies from 2% (RCA-GUESS) to 18% (RRCM).

The frequency distributions of cyclone depth and size (Figure 5) show that shallow and small cyclones occur most often. The across-model variation is, in general, small for both nudged and unnudged models in both seasons. But substantial variations across the models occur for shallow cyclones (depth of up to 4 hPa) and for small cyclones (radius of up to 400 km) for both seasons. However, the nudged models show less variation compared to the unnudged models.

3.1.3. Intercomparison of ASR With Other Reanalyses

Recent results from the analysis of cyclone activity in the Arctic using high-resolution ASR have shown an advantage of this reanalysis relative to global reanalyses (Smirnova & Golubkin, 2017; Tilinina et al., 2014). ASR is not employed to the same degree as the four more widely used reanalyses in this study due to its

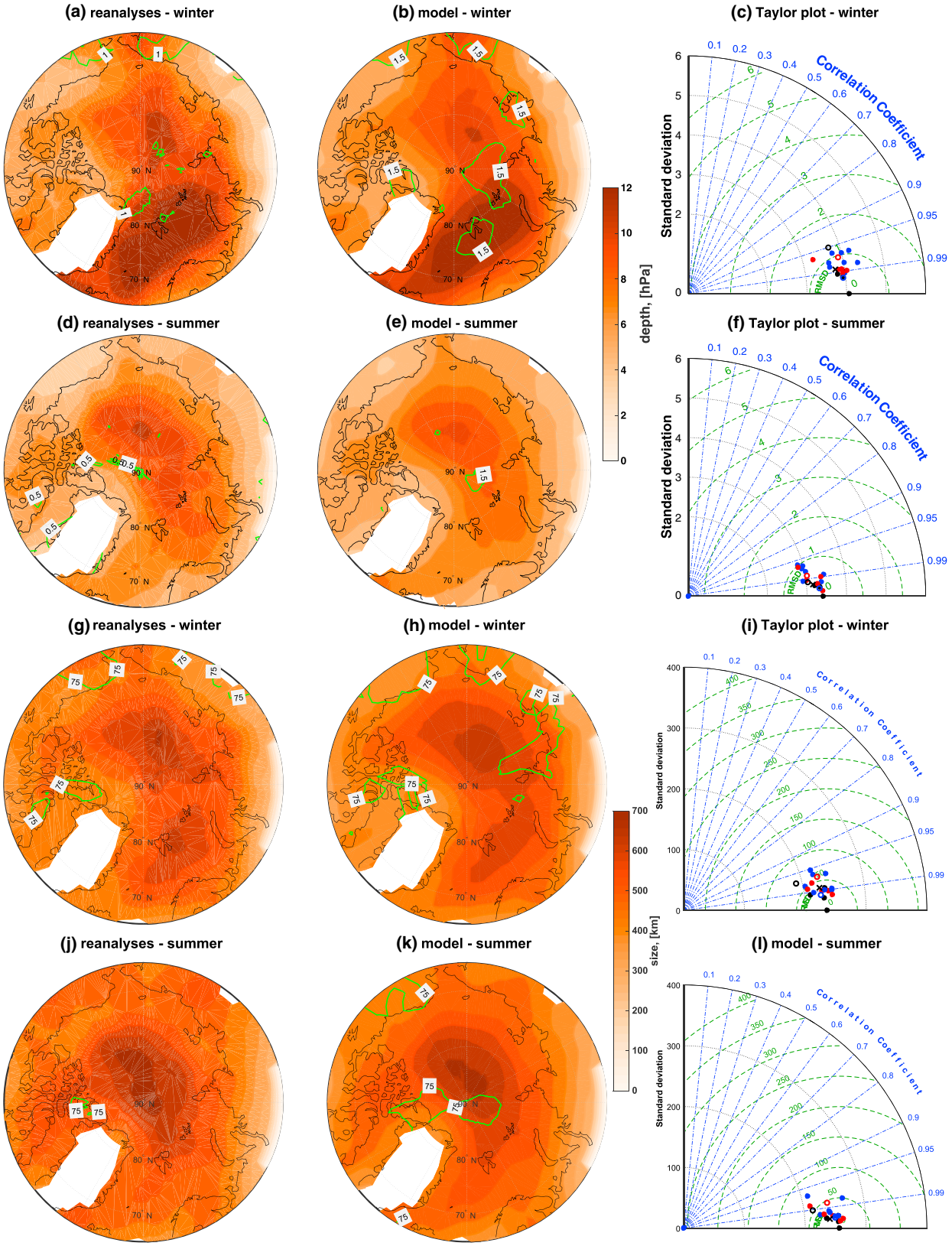

Figure 4. Spatial distribution of (a, b, d, and e) cyclone mean depth (hPa) and (g, h, j, and k) size (km) in (a, b, g, and h) winter and (d, e, j, and k) summer from multireanalysis and multimodel ensemble. The green isolines indicate the standard deviations across the models or reanalyses. Taylor plots for (c and f) depth and (i and l) size are also given (same legend as in Figure 1).

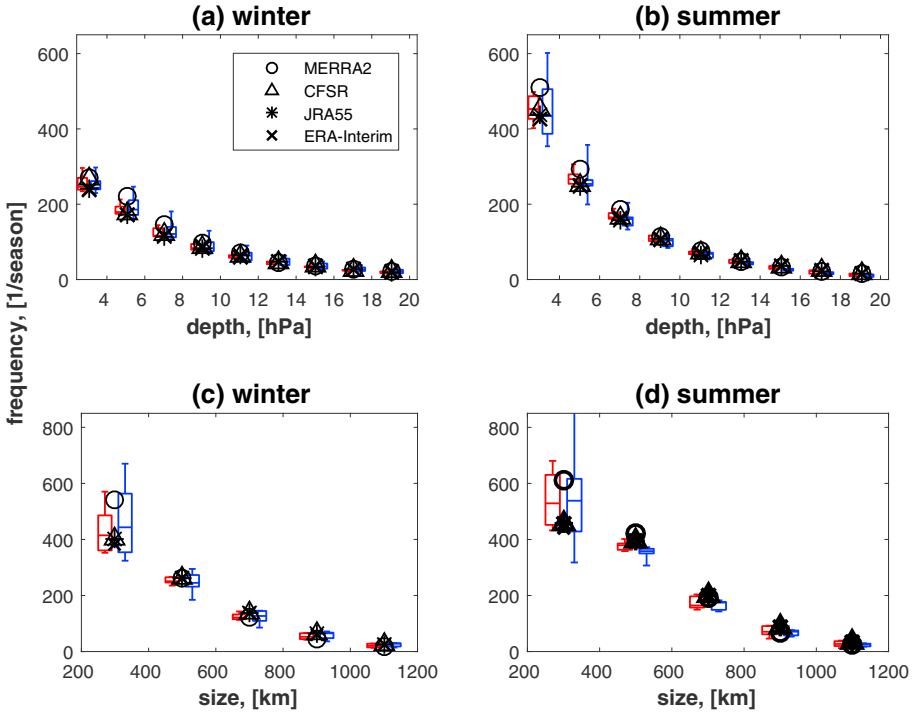

Figure 5. Frequency distribution of (a and b) cyclone depth and (c and d) size in winter and summer from multireanalysis data and multimodel ensemble (nudged [red] and nonnudged [blue]). The latter is given in box-whisker format and shows the minimum and maximum values, the lower and upper quartiles, and the median.

short time period (2000–2012). However, it is illuminating to compare results from ASR with those based on the four reanalyses adopted in this study.

Here we compare cyclone characteristics obtained from ASR and ERA-Interim reanalyses. Given the limited period of ASR reanalysis, we analyzed the cyclone climatology from both reanalyses for the overlapping period. Tilinina et al. (2014) noted a considerably higher number of cyclones over the Arctic with the largest differences over land using the previous version of ASR reanalysis. We also get similar results using the latest version of ASR. As we mentioned above, ASR shows the highest cyclone frequency relative to ERA-Interim for both seasons, in particular over land (Figure 2). However, cyclone frequency over ocean is underestimated in winter and slightly overestimated in summer by ASR relative to ERA-Interim. This discrepancy is related to smaller cyclones, which are excluded from our analysis. However, if we remove the restrictions on cyclone size, we obtain the highest cyclone frequency over ocean in winter. This indicates that ASR counts for more small (and shallow) cyclones compared to ERA-Interim. ASR underestimates the number of deep cyclones and overestimates cyclone mean depth over land in winter compared to ERA-Interim. In summer, ASR shows less cyclone frequency only over ocean. It should also be noted that values of 95th percentile for cyclone depth distribution in case of ASR and ERA-Interim reanalyses differ by ~25% (ASR shows lower value for deep cyclones than any other reanalyses).

Taylor diagrams showing spatial correlations between cyclone frequency from ASR and other reanalyses for the 2000–2010 period are presented in supporting Figure S1. The spatial correlation coefficients between the ASR and individual reanalyses for cyclone frequency are lower in winter and ranges from 0.75 (JRA55) to 0.84 (MERRA2) with corresponding standard deviations (5.0–5.6) and RMSEs (3.2–3.8) (cyclones per season). In summer, correlations are high and ranges from 0.94 (CFSR) to 0.97 (MERRA2) (Figure S1) with *SD*s (6.9–7.2) and RMSEs (1.6–2.5). Therefore, MERRA2 is more closest to ASR than other reanalyses. Both reanalyses show highest number of cyclones in both seasons.

3.2. Trends in Cyclone Characteristics

The analysis of the 30 year (1981–2010) trends in cyclone frequency shows that most models simulate a decrease for winter and summer, but these trends are not statistically significant (Figure 6a). In contrast,

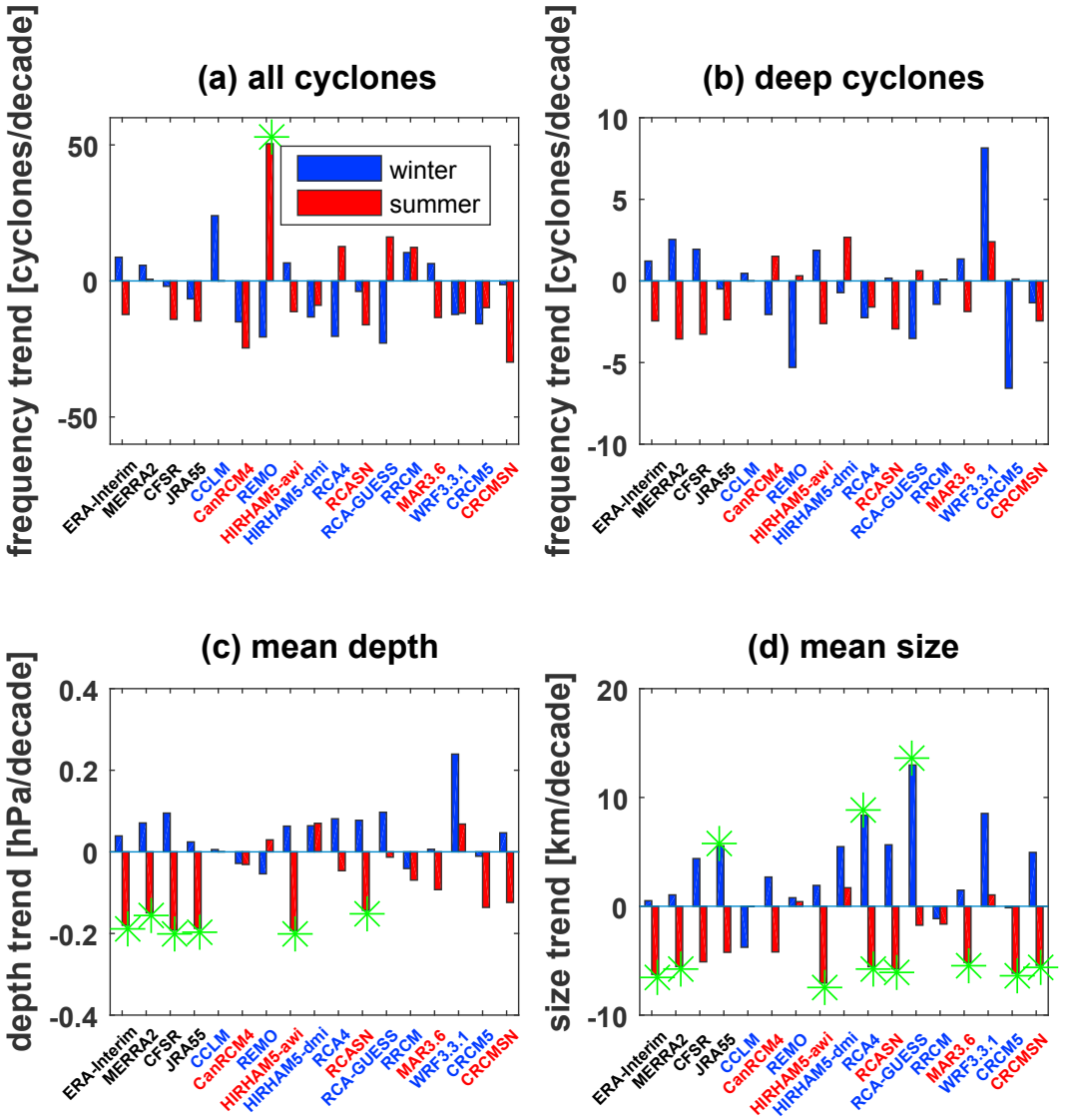

Figure 6. Thirty-year trends (1981–2010) of cyclone frequency for (a) all cyclones, (b) deep cyclones, (c) cyclone mean depth, and (d) size from reanalyses and models in winter (blue) and summer (red), averaged over the Arctic. The green asterisks show statistical significance at $p < 0.1$. The names of the different data sets on the x axis are highlighted by color (black, reanalyses; red, nudged models; blue, nonnudged models).

the reanalyses disagree with each other. In winter, two of them show an increase, whereas the other two exhibit a decrease. In summer, most (three of four) show negative trends. The nudged models demonstrate a different behavior in both seasons: three models (CanRCM4, RCA4, and CRCMSN) show the same trend signs as ERA-Interim and the other two models agree with CFSR and JRA55. Only four (out of seven) models without nudging show the same behavior as in reanalyses.

Most reanalyses show consistent trends for the frequency of deep cyclones (Figure 6b), with an increase in winter and a decrease in summer. Conversely, most of the models show a decrease in winter and an increase in summer for deep cyclones. Three nudged models show the same trend as the most reanalyses for both seasons. However, trend signs from one (CRCMSN) nudged model are similar to JRA55. Most unnudged models show different trend signs. However, some outliers are observed for all and for deep cyclones. For all cyclones, the strongest positive (REMO) and negative (CanRCM4 and CRCMSN) trends are observed in summer. In the case of deep cyclones, the strongest trends are noted in winter: positive in WRF3.3.1 and negative in CRCM5. None of the trends in deep cyclones are statistically significant.

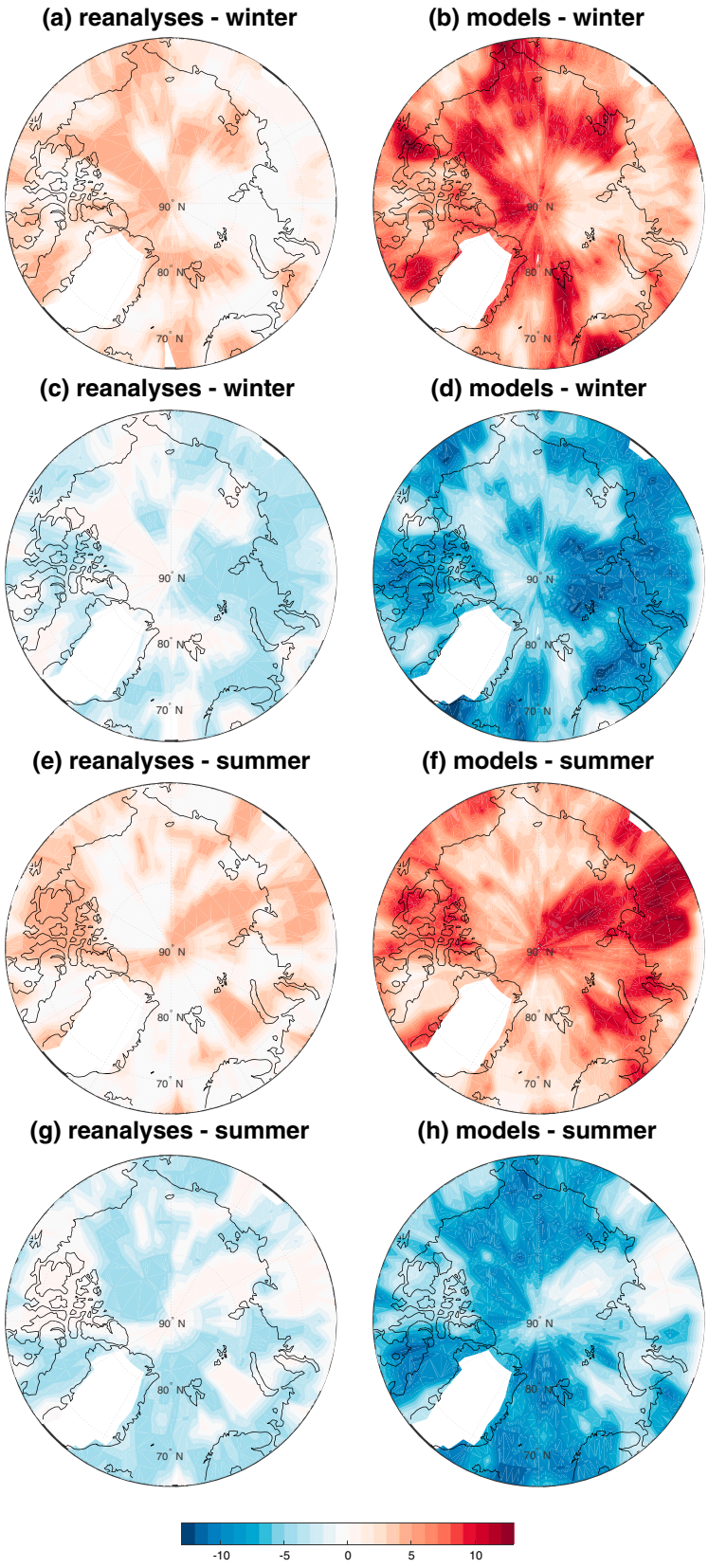

Figure 7. Number of data sets showing positive or negative cyclone frequency trend (1981–2010) in (a–d) winter and (e–h) summer. The color scale represents the number of data sets with a positive (red colors) and negative (blue colors) trends.

Table 2
Spatial Correlation Coefficients for Cyclone Characteristic Trends (Winter/Summer) From RCMs (Nudged Models—Italic) and ERA-Interim for Winter and Summer (Where Orange >0.5, Green >0.7, and Red >0.9)

	MERRA2	CFSR	JRA55	CCLM	*CanRCM4*	REMO	*HIRHAM5-AWI*	HIRHAM5-dmi	RCA4	*RCASN*	RCA-GUESS	RRCM	*MAR3.6*	WRF3.3.1	CRCM5	*CRCMSN*
Cyclone fr.	0.79/0.78	0.82/0.86	0.78/0.89	0.80/–	**0.50**/0.38	0.10/0.01	**0.94/0.95**	0.13/0.32	0.10/0.25	**0.61**/0.84	−0.01/0.24	0.35/−0.25	0.77/0.82	0.10/0.37	−0.14/0.15	0.48/**0.52**
Mean depth	**0.58/0.68**	**0.68/0.67**	**0.64**/0.81	**0.63**/–	0.10/−0.01	0.25/−0.17	0.79/0.86	0.07/−0.07	−0.25/0.04	0.43/**0.65**	0.12/−0.11	−0.09/0.09	**0.51/0.51**	−0.09/−0.29	0.20/0.23	0.30/0.39
Mean size	**0.52/0.63**	**0.54/0.56**	0.46/0.75	**0.52**/–	0.06/−0.01	0.11/−0.06	**0.60**/0.80	0.04/−0.14	−0.04/−0.12	0.30/**0.65**	0.06/−0.28	−0.01/−0.18	0.34/**0.54**	−0.09/−0.27	0.14/0.38	0.26/0.24

Note. RCM = regional climate model; MERRA-2 = Modern-Era Retrospective analysis for Research and Applications Version 2; CFSR = Climate Forecast System Reanalysis; JRA 55 = Japanese 55-year reanalysis; CCLM = COSMO Climate Limited-area Model; CanRCM4 = Canadian Centre for Climate Modelling and Analysis Regional Climate Model version 4; REMO = RCM REMO (REgional MOdel); HIRHAM5-AWI = Alfred Wegener Institute (AWI) RCM HIRHAM version 5; RCA4 - The Rossby Centre RCM; HIRHAM5-dmi - Danish Meteorological Institute (DMI) RCM HIRHAM version 5; RCASN = RCM RCA4 with spectral nudging; RCA-GUESS = RCM RCA4 coupled with dynamic vegetation and ecosystem biogeochemistry simulated by the vegetation-ecosystem model LPJ-GUESS; RRCM = Voeikov Main Geophysical Observatory RCM; MAR3.6 = RCM MAR version 3.6; WRF3.3.1 = Weather Research and Forecasting version 3.3.1; CRCM5 = Canadian Regional Climate Model; CRCMSN = RCM CRCM5 with spectral nudging.

The trends for cyclone mean depth are consistent across the reanalyses. However, only half (including four models with nudging) of the models show the same trend signs for both seasons (Figure 6 c). They show a small increase in winter and a decrease in summer. The summer trends are significant for 2 of the 13 models and for all reanalyses. The same across-model and reanalysis agreement is seen for the trend in cyclone mean size: increase in winter and decrease in summer. And, the majority of the models (five nudged and two unnudged) show similar trends as in the reanalyses.

Figure 7 shows the agreement in the spatial patterns of trends for cyclone frequency in both seasons. The model patterns agree with the reanalyses on key regional trends. In winter, they show an increase over Norwegian Sea, Davis Strait, Spitsbergen region, Laptev Sea, and north of the Canadian Archipelago and a decrease over the Barents and Kara Seas, Greenland Sea, and over the southeast of Greenland. In summer, they agree on an increase over the Barents Sea, parts of Kara Sea and Laptev Sea, over the Canadian Archipelago, and over parts of eastern Siberia and a decrease in the Baffin Bay, Greenland and Norwegian Seas, and East Siberian, Chukchi, and Beaufort Seas. Discrepancies between models' and reanalyses' trends of cyclone mean depth and size in winter (Supporting Figures S2 and S3) arise over the Norwegian Sea. Reanalyses show an increase of cyclone mean depth and size over this region, whereas most of the models show a decrease.

Spatial correlation coefficients for cyclone frequency trends between RCMs and ERA-Interim range from 0.48/0.38 (CRCM5/CanRCM4) to 0.94/0.95 (HIRHAM5-AWI) for the nudged models and from −0.01/−0.25 (RCA-GUESS/RRCM) to 0.80/0.37 (CCLM/WRF3.3.1) for the unnudged models for winter/summer (Table 2). Most models with SN reproduce the spatial trends of cyclone characteristics reasonably well. It should be noted that spatial correlation for all cyclone characteristics trends in case of reanalyses is higher for both seasons in comparison with the majority of the models.

One of the reasons leading to the differences in cyclone characteristics and their trends described above may be related to the representation of zonal wind in the troposphere, in particular the jet stream. Some authors (e.g., Pinto et al., 2007; Zappa et al., 2013) stressed a significant role of the jet stream in representing cyclone activity over the North Atlantic in GCMs. Berg et al. (2013) indicated a key role of nudging in RCMs for reducing the biases in the free troposphere and the MSLP. Our results also confirm that most models with nudging accurately reproduce both the spatial pattern of cyclone characteristics and their trends. However, only three out of five nudged models can reproduce spatial trends correctly for all cyclone characteristics (Table 2). The other two nudged models (CanRCM4 and CRCMSN) show a high spatial correlations for cyclone frequency but lower correlations for cyclone mean depth and size. These models nudged the winds, whereas the other models additionally also nudged the temperature at different levels (Table 1). This led to improved cyclone representation and their changes. Although CCLM was not nudged, it was run in a forecasting procedure; that is, it started every day with new initial conditions from ERA-Interim (and external sea-ice fields) without nudging during a day-long simulation (see, e.g., Lucas-Picher et al., 2013). With such

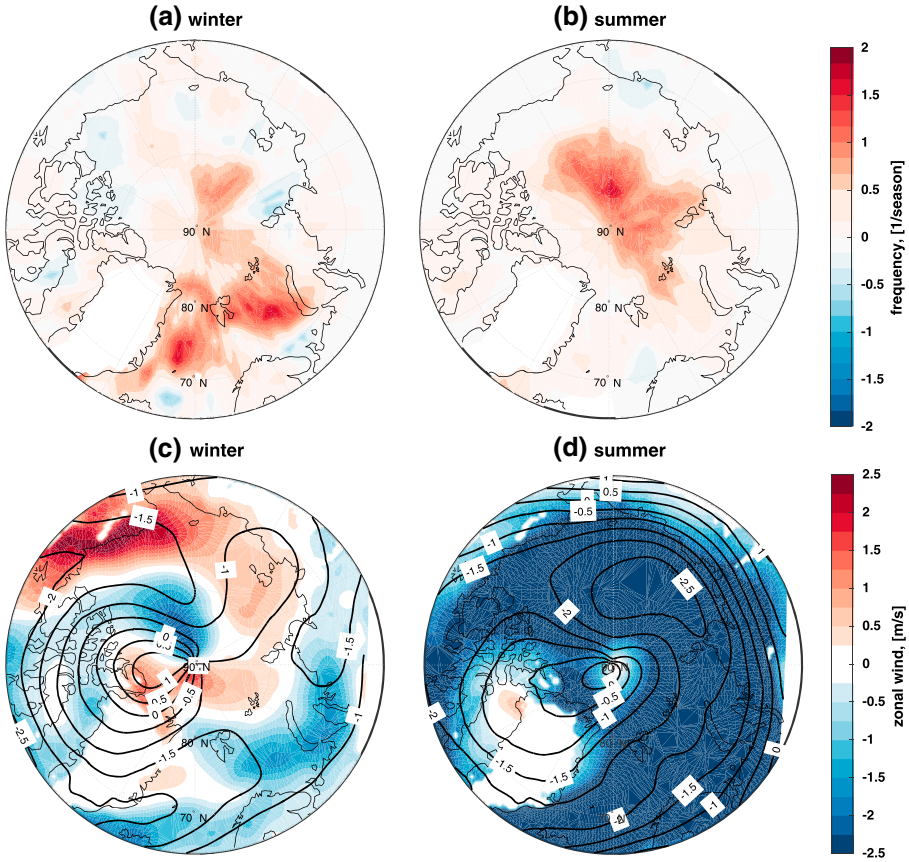

Figure 8. Differences "RCASN minus RCA" in spatial distribution of (a and b) deep cyclone frequency and of (c and d) u850 (m/s) in winter and summer for the period 1981–2010. The black isolines in (c and d) indicate differences of u200 (m/s).

a setup, CCLM could not drift far from ERA-Interim. Therefore, this might explain the high correlations with the reanalysis.

The primary factor affecting the generation and evolution of cyclones in high latitudes is the baroclinicity of the atmosphere. There are two factors influencing the baroclinicity and cyclone activity—Brunt-Väisälä frequency, which is related to the vertical temperature gradient and is a measure of stratification, and vertical wind shear, which is related to the horizontal temperature gradient. Therefore, a possible explanation of intramodel differences is that a different representation of the vertical and horizontal temperature distribution in the models may change the stability in the atmosphere and, hence, impact on cyclone characteristics and their variability in the Arctic. For instance, the Rossby radius (cyclone size) depends only on a vertical stratification of the temperature (Brunt-Väisälä frequency) and is connected with cyclone depth (e.g., Golitsyn et al., 2007). This explains the impact of temperature nudging on simulated cyclone characteristics. But to investigate the specific impacts of nudging, dedicated experiments with different nudged variables are needed.

3.3. Impacts of Nudging Applied to Cyclone Characteristics

To examine the connection of atmospheric circulation fields with cyclone activity representation in the Arctic, we compared 850 hPa (U850) and 200 hPa (U200) winds simulated by the Arctic CORDEX models with ERA-Interim data. Evaluation of the winds shows that the spatial correlations between the nudged models and ERA-Interim for U850 vary from 0.5/0.8 (MAR3.6) to 0.6/0.9 (HIRHAM5-AWI) for winter/summer. In case of U200, the spatial correlations are higher for all RCMs and exceed 0.9 (only MAR3.6 shows $R = 0.8$) for both seasons. As expected, the models without nudging (excluding CCLM which shows high correlations for both seasons) have lower spatial correlation overall, in particular for upper-level zonal wind.

We find a significant connection between the zonal wind and the frequency of deep cyclones and cyclone mean depth over the Arctic. Correlation between U200 and frequency of deep cyclones among all models

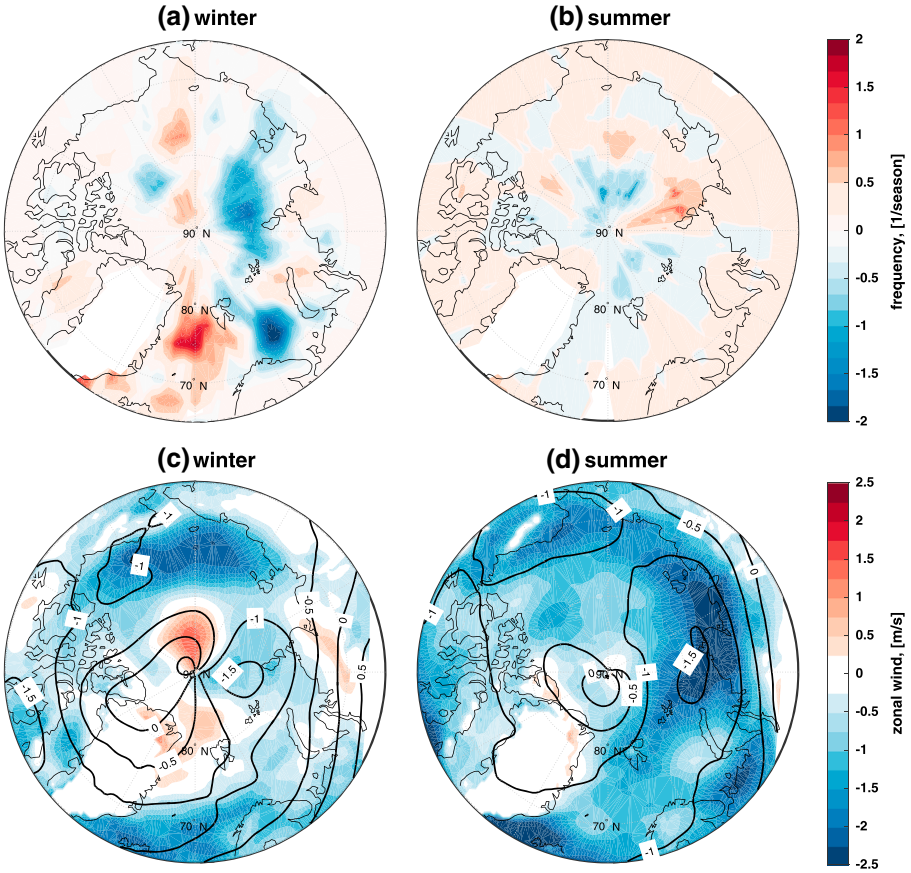

Figure 9. As Figure 8 but for "CRCMSN minus CRCM."

is statistically significant ($R \sim 0.5$) and higher than for U850 in winter. In summer, statistically significant positive correlation is found between U200 and cyclone mean depth. It should be noted that zonal winds at 200 and 850 hPa are underestimated in most of the models compared to ERA-Interim, which possibly leads to an underestimation in cyclone mean depth and frequency of deep cyclones in the Arctic.

The cyclone characteristics from the nudged models relative to ERA-Interim show fewer differences than the unnudged ones, in particular in summer (Figure 2). However, large intraensemble variability for deep cyclones occurs. Some models (CanRCM4 and MAR3.6) with nudging show no differences in the analyzed characteristics for all cyclones in both seasons but they differ in representation of deep cyclones in winter. CRCM5 and CRCMSN show almost no differences for the cyclone characteristics in winter. It seems that CRCM5 reproduces the cyclone activity quite well, in particular the atmospheric circulation when compared to ERA-Interim. Thus, the additional nudging applied to CRCM5 cannot further improve the results as much as in RCA4. In summer, most models, including the nudged models (CanRCM4, HIRHAM5-AWI, RCASN, and MAR3.6) underestimate the deep cyclone occurrence.

To better understand the role of nudging in representing cyclone characteristics, we focus here on the two models that were run with SN and without nudging, namely, RCA and RCASN, and CRCM5 and CRCMSN, respectively. CRCMSN only nudges wind fields, whereas in RCASN both wind and temperature fields are nudged (see Table 1).

RCA4 and RCASN show small differences in cyclone frequency compared to ERA-Interim for both seasons (Figure 2). However, RCA4 underestimates the frequency of deep cyclones with respect to RCASN for both seasons, while RCASN is in a better agreement with ERA-Interim. Thus, SN improves deep cyclone representation over the Arctic, particularly in summer. In summer, the model differences occur over the Arctic Ocean, while in winter, it occurs along the sea-ice edge over the area between Greenland and Barents Sea (Figures 8a and 8b). We analyzed the 200 and 850 hPa zonal wind from both versions of the model (Figures 8c and 8d). In winter, in the area of deep cyclone activity in the Nordic Seas, RCASN simulates stronger U200 and U850

winds compared to RCA4. The same is seen over the central Arctic Ocean in summer. RCASN wind is in a close agreement with ERA-Interim. The spatial correlation coefficients between the RCASN and ERA-Interim zonal winds for the two levels are a bit higher (R = 0.94 and 0.65 in winter, R = 0.88 and 0.92 in summer) than in the case of RCA4 (R = 0.93 and 0.63 in winter, R = 0.82 and 0.80) for both seasons. This confirms a connection between the strength of the zonal wind and deep cyclone frequency, which has been discussed previously (e.g., Seiler & Zwiers, 2016; Zappa et al., 2013).

CRCM does not show such big differences with and without nudging. CRCM5 and CRCMSN show approximately the same differences for all and deep cyclone frequency compared to ERA-Interim for both seasons (Figure 2). It seems that the nudging does not influence the overall cyclone frequency in this model, but it affects their spatial distribution. (Figure 9). CRCM5 overestimates the frequency of deep cyclones (relative to CRCMSN) over the Barents and Laptev Seas and underestimates it over the Southeast Greenland and over the Greenland Sea in winter. In summer, CRCM5 overestimates the frequency of deep cyclones over the central Arctic Ocean and underestimates it over the Laptev Sea. Compared to CRCMSN, CRCM5 overestimates the 200 and 850 hPa zonal wind almost everywhere in the Arctic. However, the amplitude of change is small.

4. Summary and Conclusion

The ability of the RCMs participating in the Arctic CORDEX to simulate the cyclone activity in the Arctic region in comparison with reanalysis data is assessed. Different characteristics of cyclone activity are intercompared in the ensemble of RCMs hindcast simulations and multireanalysis data (ERA-Interim, NCEP-CFSR, NASA-MERRA2, and JMA-JRA55) for winter and summer during the 1981–2010 period. Biases in cyclone frequency, intensity, and size over the Arctic (region ~north of 65°N) are quantified.

The majority of the models accurately reproduce the spatial distribution of cyclone characteristics (frequency, mean depth, and size) when compared to reanalysis data. The models are able to reproduce the distributions of the mean depth and size of the deepest cyclones in the region between Greenland and Barents Sea in winter and over the central Arctic in summer and the largest cyclones over the eastern part of the Arctic Ocean during both seasons. The strongest variations in cyclone frequency among the reanalysis and model data are observed over the Baffin Bay, Foxe Basin, and over Eastern Siberia in winter and additionally over the Queen Elizabeth Islands and Alaska in summer. It is related to small and shallow cyclones (depth up to 4 hPa and radius up to 400 km) for both seasons.

Generally, there are many factors that affect the intramodel differences. (i) Differences in cyclone frequency across the models are observed over areas with complex coastlines and orography in both seasons. It is known that orographic forcing plays an important role in cyclone formation and its life cycle, as well as in shaping the jets (e.g., Brayshaw et al., 2009; Kristjansson & McInnes, 1999; Tsukernik et al., 2007). (ii) Sea-ice concentration and thickness play a significant role in changing the heat transfer between the ocean and atmosphere in high latitudes, leading to changes of large-scale atmospheric circulation, vertical stability, and therefore cyclone activity changes (Inoue et al., 2008; Jaiser et al., 2012; Lang et al., 2017; Semenov & Latif, 2015). Vertical stability can also influence polar mesoscale circulation, particularly for the polar lows. Polar lows are intense polar mesocyclones that are characterized by a short lifetime (less than one day) and a relatively small size (diameter less than 1,000 km). They form during the cold seasons over relatively warm ocean surface (Heinemann & Claud, 1997; Mokhov et al., 2007). For instance, differences in the number of polar lows in GCMs are associated with the differences in mean vertical stability (Zahn & von Storch, 2010). In case of regional models, the reason for differences in cyclone characteristics across the models may also be due to incorrect representation of physical processes at regional scales, particularly at the mesoscale, which influences the background conditions of cyclone genesis and growth. (iii) Land-sea contrast, which can vary depending on a model's land-surface scheme, can also influence the cyclone activity. In summer, when cyclone activity occurs over land, and a heating contrast between the Eurasian continent and Arctic Ocean develops (e.g., Serreze & Barrett, 2008), this mechanism plays a significant role. In winter, thermal contrasts develop between relatively warm open ocean water (North Atlantic drift) and the Greenland ice sheet. Such gradients can help to support cyclone development in this area (including mesoscale polar cyclones) (Serreze et al., 1993, 1997).

Most Arctic-CORDEX models show an insignificant decrease of cyclone frequency in winter and summer. The reanalyses also show disagreements, particularly in winter. The frequency of deep cyclones, however,

significantly increases (decreases) for the reanalyses in winter (summer), but models exhibit mixed results. Trends for cyclone mean depth and size are characterized by an increase in winter and decrease in summer. These changes are significant for 2 of the 13 model simulations and for all reanalyses. Furthermore, the models agree with the reanalyses on the key regional spatial trend patterns.

We find significant connections between zonal wind and the frequency of deep cyclones and cyclone mean depth over the Arctic. Our results show that an underestimation of zonal winds in RCMs compared to ERA-Interim may lead to underestimation in cyclone mean depth and frequency of deep cyclones in the Arctic.

The intercomparison reveals that RCMs with large-scale spectral wind nudging represent the cyclone activity characteristics in the Arctic region much better due to the forced representations of zonal winds as expected. Biases are further reduced by additional nudging of temperature. Hence, along with previous studies, we speculate that nudged variables and nudging strength may play a significant role in the representation of cyclone characteristics and trends, in particular, cyclone depth and size over the Arctic region.

Acknowledgments
M. A., I. I. M., V. A. S., M. A. D., A. R., and K. D. acknowledge the support by the project "Quantifying Rapid Climate Change in the Arctic: regional feedbacks and large-scale impacts (QUARCCS)" funded by the German and Russian Ministries of Research and Education. A. R. and K. D. acknowledge the support by the SFB/TR172 "ArctiC Amplification: Climate Relevant Atmospheric and SurfaCe Processes, and Feedback Mechanisms $(AC)^3$" funded by the Deutsche Forschungsgemeinschaft (DFG). V. A. S., and M. A. D. were also supported by Russian Science Foundation (grant 14-17-00647). M. A., and I. I. M. was partly supported by Russian Science Foundation (grant 14-17-00806) with the use of results obtained under the frames of RFBR projects and RAS programs. The CCLM contribution to Arctic-CORDEX was partly funded by the German Federal Ministry of Education and Research (BMBF) under grant 03G0833D. The HIRHAM-dmi contribution to Arctic-CORDEX leading to these results has received funding from the European Research Council under the European Community's Seventh Framework Programme (FP7/2007-2013)/ERC grant agreement 610055 as part of the ice2ice project. T. K. was supported by the Nordic Centre of Excellence ARCPATH "Arctic Climate Predictions: Pathways to Resilient, Sustainable Societies," funded by the Nordic Arctic Research initiative. M. A. and S. S. acknowledge Norwegian supercomputing support through projects NS9001K and NN9280K. We acknowledge the Japan Meteorological Agency (JMA) for providing JRA-55, the European Centre for Medium- Range Weather Forecasts (ECMWF) for providing ERA-Interim, the National Centers for Environmental Prediction (NCEP) for providing NCEP-CFSR, NASA Goddard Earth Sciences (GES) Data and Information Services Center (DISC) for providing MERRA2, and Polar meteorology group for providing ASR reanalysis. Data from reanalyses were retrieved from https://reanalyses.org/atmosphere/overview-current-atmospheric-reanalyses/. We thank the Arctic CORDEX community (listed in Table of this paper) for producing and making available their model output. We also would like to thank David Bromwich, Ohio State University, and anonymous reviewer for in-depth comments on an earlier version of this manuscript. D. Sein was supported by the state assignment of FASO Russia (theme No. 0149-2018-0014).

References

Akperov, M., Mokhov, I., Rinke, A., Dethloff, K., & Matthes, H. (2015). Cyclones and their possible changes in the Arctic by the end of the twenty first century from regional climate model simulations. *Theoretical and Applied Climatology*, *122*(1-2), 85–96. https://doi.org/10.1007/s00704-014-1272-2

Akperov, M. G., Bardin, M. Y., Volodin, E. M., Golitsyn, G. S., & Mokhov, I. I. (2007). Probability distributions for cyclones and anticyclones from the NCEP/NCAR reanalysis data and the INM RAS climate model. *Izvestiya Atmospheric and Oceanic Physics*, *43*(6), 705–712. https://doi.org/10.1134/S0001433807060047

Akperov, M. G., & Mokhov, I. I. (2010). A comparative analysis of the method of extratropical cyclone identification. *Atmospheric and Oceanic Physics*, *46*(5), 574–590. https://doi.org/10.1134/S0001433810050038

Akperov, M. G., & Mokhov, I. I. (2013). Estimates of the sensitivity of cyclonic activity in the troposphere of extratropical latitudes to changes in the temperature regime. *Izvestiya Atmospheric and Oceanic Physics*, *49*(2), 113–120. https://doi.org/10.1134/S0001433813020035

Bardin, M. Y., & Polonsky, A. B. (2005). North Atlantic oscillation and synoptic variability in the European-Atlantic region in winter. *Izvestiya Atmospheric and Oceanic Physics*, *41*(3), 127–136.

Berg, P., Döscher, R., & Koenigk, T. (2013). Impacts of using spectral nudging on regional climate model RCA4 simulations of the Arctic. *Geoscientific Model Development*, *6*(3), 849–859. https://doi.org/10.5194/gmd-6-849-2013

Brayshaw, D. J., Hoskins, B. J., & Blackburn, M. (2009). The basic ingredients of the North Atlantic storm track. Part I: Land–sea contrast and orography. *Journal of the Atmospheric Sciences*, *66*(9), 2539–2558. https://doi.org/10.1175/2009JAS3078.1

Bromwich, D. H., Wilson, A. B., Bai, L., Liu, Z., Barlage, M., Shih, C.-F., et al. (2017). The Arctic System Reanalysis Version 2. *Bulletin of the American Meteorological Society*. https://doi.org/10.1175/BAMS-D-16-0215.1

Brümmer, B., Thiemann, S., & Kirchgáßner, A. (2000). A cyclone statistics for the Arctic based on European Centrere-analysis data. *Meteorology and Atmospheric Physics*, *75*(3-4), 233–250. https://doi.org/10.1007/s007030070006

Chernokulsky, A. V., Esau, I., Bulygina, O. N., Davy, R., Mokhov, I. I., Outten, S., & Semenov, V. A. (2017). Climatology and interannual variability of cloudiness in the Atlantic Arctic from surface observations since the late 19th century. *Journal of Climate*, *30*(6), 2103–2120. https://doi.org/10.1175/JCLI-D-16-0329.1

Christensen, J. H., Krishna Kumar, K., Aldrian, E., An, S.-I., Cavalcanti, I. F. A., de Castro, M., et al. (2013). Climate phenomena and their relevance for future regional climate change. In T. F. Stocker, et al. (Eds.), *Climate Change 2013: The Physical Science Basis. Contribution of Working Group I to the Fifth Assessment Report of the Intergovernmental Panel on Climate Change* (pp. 1217–1308). Cambridge, United Kingdom and New York: Cambridge University Press. https://doi.org/10.1017/CBO9781107415324.028

Christensen, O. B., Drews, M., Christensen, J. H., Dethloff, K., Ketelsen, K., Hebestadt, I., & Rinke, A. (2007). DMI technical report, 06–17, The HIRHAM Regional Climate Model Version 5 (β).

Côté, H., Grise, K. M., Son, S. W., de Elía, R., & Frigon, A. (2015). Challenges of tracking extratropical cyclones in regional climate models. *Climate Dynamics*, *44*(11-12), 3101–3109. https://doi.org/10.1007/s00382-014-2327-x

Crawford, A. D., & Serreze, M. C. (2016). Does the summer arctic frontal zone influence arctic ocean cyclone activity? *Journal of Climate*, *29*(13), 4977–4993. https://doi.org/10.1175/JCLI-D-15-0755.1

Dee, D. P., Uppala, S. M., Simmons, A. J., Berrisford, P., Poli, P., Kobayashi, S., et al. (2011). The ERA-Interim reanalysis: Configuration and performance of the data assimilation system. *Quarterly Journal of the Royal Meteorological Society*, *137*(656), 553–597. https://doi.org/10.1002/qj.828

Ebita, A., Kobayashi, S., Ota, Y., Moriya, M., Kumabe, R., Onogi, K., et al. (2011). The Japanese 55-year Reanalysis "JRA-55": An interim report. *SOLA*, *7*, 149–152. https://doi.org/10.2151/sola.2011-038

European Organisation for the Exploitation of Meteorological Satellites (2015). Global sea ice concentration reprocessing dataset 1978-2015 (v1.2, 2015). Norwegian and Danish Meteorological Institutes. Retrieved from http://osisaf.met.no

Fettweis, X., Box, J. E., Agosta, C., Amory, C., Kittel, C., Lang, C., et al. (2017). Reconstructions of the 1900–2015 Greenland ice sheet surface mass balance using the regional climate MAR model. *The Cryosphere*, *11*, 1015–1033. https://doi.org/10.5194/tc-11-1015-2017

Gelaro, R., McCarty, W., Suárez, M. J., Todling, R., Molod, A., Takacs, L., et al. (2017). The Modern-Era Retrospective Analysis for Research and Applications, Version 2 (MERRA-2). *Journal of Climate*, *30*(14), 5419–5454. https://doi.org/10.1175/JCLI-D-16-0758.1

Golitsyn, G. S., Mokhov, I. I., Akperov, M. G., & Bardin, M. Y. (2007). Distribution functions of probabilities of cyclones and anticyclones from 1952 to 2000: An instrument for the determination of global climate variations. *Doklady Earth Sciences*, *413*(1), 324–326. https://doi.org/10.1134/S1028334X07020432

Gutjahr, O., Heinemann, G., Preußer, A., Willmes, S., & Drüe, C. (2016). Quantification of ice production in Laptev Sea polynyas and its sensitivity to thin-ice parameterizations in a regional climate model. *The Cryosphere*, *10*, 2999–3019. https://doi.org/10.5194/tc-2999-2016

Heinemann, G., & Claud, C. (1997). Report of a workshop on "Theoretical and observational studies of POLAR lows" of the EUROPEAN GEOPHYSICAL SOCIETY POLAR LOWS WORKING GROUP. *Bulletin of the American Meteorological Society*, *78*, 2643–2658.

Inoue, J., Curry, J. A., & Maslanik, J. A. (2008). Application of aerosondes to melt-pond observations over Arctic Sea ice. *Journal of Atmospheric and Oceanic Technology*, *25*(2), 327–334. https://doi.org/10.1175/2007JTECHA955.1

Inoue, J., Hori, M. E., & Takaya, K. (2012). The role of Barents Sea ice in the wintertime cyclone track and emergence of a warm-Arctic cold-Siberian anomaly. *Journal of Climate*, *25*(7), 2561–2568. https://doi.org/10.1175/JCLI-D-11-00449.1

Jaiser, R., Dethloff, K., Handorf, D., Rinke, A., & Cohen, J. (2012). Impact of sea ice cover changes on the northern hemisphere atmospheric winter circulation. *Tellus Series A: Dynamic Meteorology and Oceanography*, *64*(1), 1–11. https://doi.org/10.3402/tellusa.v64i0.11595

Klaus, D., Dethloff, K., Dorn, W., Rinke, A., & Wu, D. L. (2016). New insight of Arctic cloud parameterization from regional climate model simulations, satellite-based, and drifting station data. *Geophysical Research Letters*, *43*, 5450–5459. https://doi.org/10.1002/2015GL067530

Kobayashi, S., Ota, Y., Harada, Y., Ebita, A., Moriya, M., Onoda, H., et al. (2015). The JRA-55 Reanalysis: General specifications and basic characteristics. *Journal of the Meteorological Society of Japan*, *93*(1), 5–48. https://doi.org/10.2151/jmsj.2015-001

Koenigk, T., Berg, P., & Döscher, R. (2015). Arctic climate change in an ensemble of regional CORDEX simulations. *Polar Research*, *34*(1), 24603. https://doi.org/10.3402/polar.v34.24603

Kolstad, E. W., & Bracegirdle, T. J. (2016). Sensitivity of an apparently hurricane-like polar low to sea surface temperature. *Quarterly Journal of the Royal Meteorological Society*, *143*(703), 966–973. https://doi.org/10.1002/qj.2980

Koyama, T., Stroeve, J., Cassano, J., & Crawford, A. (2017). Sea ice loss and Arctic cyclone activity from 1979 to 2014. *Journal of Climate*. https://doi.org/10.1175/JCLI-D-16-0542.1

Kriegsmann, A., & Brümmer, B. (2014). Cyclone impact on sea ice in the central Arctic Ocean: A statistical study. *The Cryosphere*, *8*(1), 303–317. https://doi.org/10.5194/tc-8-303-2014

Kristjansson, J. E., & McInnes, H. (1999). The impact of Greenland on cyclone evolution in the North Atlantic. *Quarterly Journal of the Royal Meteorological Society*, *125*(560), 2819–2834. https://doi.org/10.1002/qj.49712556003

Laffineur, T., Claud, C., Chaboureau, J.-P., & Noer, G. (2014). Polar lows over the Nordic Seas: Improved representation in ERA-Interim compared to ERA-40 and the impact on downscaled simulations. *Monthly Weather Review*, *142*(6), 2271–2289. https://doi.org/10.1175/MWR-D-13-00171.1

Lang, A., Yang, S., & Kaas, E. (2017). Sea ice thickness and recent Arctic warming. *Geophysical Research Letters*, *44*, 409–418. https://doi.org/10.1002/2016GL071274

Lucas-Picher, P., Boberg, F., Christensen, J. H., & Berg, P. (2013). Dynamical downscaling with reinitializations: A method to generate fine-scale climate data sets suitable for impact studies. *Journal of Hydrometeorology*, *14*(4), 1159–1174. https://doi.org/10.1175/JHM-D-12-063.1

Lucas-Picher, P., Wulff-Nielsen, M., Christensen, J. H., Aðalgeirsdóttir, G., Mottram, R., & Simonsen, S. B. (2012). Very high resolution regional climate model simulations over Greenland: Identifying added value. *Journal of Geophysical Research*, *117*, D02108. https://doi.org/10.1029/2011JD016267

Martynov, A., Laprise, R., Sushama, L., Winger, K., Šeparović, L., & Dugas, B. (2013). Reanalysis-driven climate simulation over CORDEX North America domain using the Canadian Regional Climate Model, version 5: Model performance evaluation. *Climate Dynamics*, *41*(11-12), 2973–3005. https://doi.org/10.1007/s00382-013-1778-9

McCabe, G. J., Clark, M. P., & Serreze, M. C. (2001). Trends in Northern Hemisphere surface cyclone frequency and intensity. *Journal of Climate*, *14*(12), 2763–2768. https://doi.org/10.1175/1520-0442(2001)014%3C2763:TINHSC%3E2.0.CO;2

Mizuta, R. (2012). Intensification of extratropical cyclones associated with the polar jet change in the CMIP5 global warming projections. *Geophysical Research Letters*, *39*, L19707. https://doi.org/10.1029/2012GL053032

Mokhov, I. I., Akperov, M. G., Lagun, V. E., & Lutsenko, E. I. (2007). Intense Arctic mesocyclones. *Izvestiya Atmospheric and Oceanic Physics*, *43*(3), 259–265. https://doi.org/10.1134/S0001433807030012

Mokhov, I. I., Chernokul'skii, A. V., Akperov, M. G., Dufresne, J.-L., & Le Treut, H. (2009). Variations in the characteristics of cyclonic activity and cloudiness in the atmosphere of extratropical latitudes of the Northern Hemisphere based from model calculations compared with the data of the reanalysis and satellite data. *Doklady Earth Sciences*, *424*(1), 147–150. https://doi.org/10.1134/S1028334X09010310

Neu, U., Akperov, M. G., Bellenbaum, N., Benestad, R., Blender, R., Caballero, R., et al. (2013). Imilast: A community effort to intercompare extratropical cyclone detection and tracking algorithms. *Bulletin of the American Meteorological Society*, *94*(4), 529–547. https://doi.org/10.1175/BAMS-D-11-00154.1

Nishii, K., Nakamura, H., & Orsolini, Y. J. (2015). Arctic summer storm track in CMIP3/5 climate models. *Climate Dynamics*, *44*(5-6), 1311–1327. https://doi.org/10.1007/s00382-014-2229-y

Orsolini, Y. J., & Sorteberg, A. (2009). Projected changes in Eurasian and Arctic summer cyclones under global warming in the Bergen climate model. *Atmospheric and Oceanic Science Letters*, *2*(1), 62–67. https://doi.org/10.1080/16742834.2009.11446776

Parkinson, C. L., & Comiso, J. C. (2013). On the 2012 record low Arctic sea ice cover: Combined impact of preconditioning and an August storm. *Geophysical Research Letters*, *40*, 1356–1361. https://doi.org/10.1002/grl.50349

Pinto, J. G., Ulbrich, U., Leckebusch, G. C., Spangehl, T., Reyers, M., & Zacharias, S. (2007). Changes in storm track and cyclone activity in three SRES ensemble experiments with the ECHAM5 / MPI-OM1 GCM. *Changes*, *29*(2-3), 195–210. https://doi.org/10.1007/s00382-007-0230-4

Rasmussen, E. A., & Turner, J. (2003). *Polar lows: Mesoscale weather systems in the polar regions* (p. 612). Cambridge University Press. https://doi.org/10.1017/CBO9780511524974

Rinke, A., Dethloff, K., Dorn, W., Handorf, D., & Moore, J. C. (2013). Simulated Arctic atmospheric feedbacks associated with late summer sea ice anomalies. *Journal of Geophysical Research: Atmospheres*, *118*, 7698–7714. https://doi.org/10.1002/jgrd.50584

Saha, S., Moorthi, S., Pan, H.-L., Wu, X., Wang, J., Nadiga, S., et al. (2010). The NCEP Climate Forecast System Reanalysis. *Bulletin of the American Meteorological Society*, *91*(8), 1015–1058. https://doi.org/10.1175/2010BAMS3001.1

Scinocca, J., Kharin, V., Jiao, Y., Qian, M., Lazare, M., Solheim, L., et al. (2016). Coordinated global and regional climate modeling. *Journal of Climate*, *29*(1), 17–35. https://doi.org/10.1175/JCLI-D-15-0161.1

Seiler, C., & Zwiers, F. W. (2016). How well do CMIP5 climate models reproduce explosive cyclones in the extratropics of the Northern Hemisphere? *Climate Dynamics*, *46*(3-4), 1241–1256. https://doi.org/10.1007/s00382-015-2642-x

Sein, D. V., Koldunov, N. V., Pinto, J. G., & Cabos, W. (2014). Sensitivity of simulated regional Arctic climate to the choice of coupled model domain. *Tellus Series A: Dynamic Meteorology and Oceanography*, *66*(1), 1–18. https://doi.org/10.3402/tellusa.v66.23966

Sein, D. V., Mikolajewicz, U., Gröger, M., Fast, I., Cabos, W., Pinto, J. G., et al. (2015). Regionally coupled atmosphere-ocean-sea ice-marine biogeochemistry model ROM: 1. Description and validation. *Journal of Advances in Modeling Earth Systems*, *7*(1), 268–304.

Semenov, V. A., & Latif, M. (2015). Nonlinear winter atmospheric circulation response to Arctic sea ice concentration anomalies for different periods during 1966–2012. *Environmental Research Letters*, *10*(5), 054020. https://doi.org/10.1088/1748-9326/10/5/054020

Šeparović, L., Alexandru, A., Laprise, R., Martynov, A., Sushama, L., Winger, K., et al. (2013). Present climate and climate change over North America as simulated by the fifth-generation Canadian regional climate model. *Climate Dynamics*, *41*(11-12), 3167–3201. https://doi.org/10.1007/s00382-013-1737-5

Sepp, M., & Jaagus, J. (2011). Changes in the activity and tracks of Arctic cyclones. *Climatic Change*, *105*(3-4), 577–595. https://doi.org/10.1007/s10584-010-9893-7

Serreze, M. C., & Barrett, A. P. (2008). The summer cyclone maximum over the central Arctic Ocean. *Journal of Climate*, *21*(5), 1048–1065. https://doi.org/10.1175/2007JCLI1810.1

Serreze, M. C., Box, J. E., Barry, R. G., & Walsh, J. E. (1993). Meteorology, and atmospheric physics characteristics of Arctic synoptic activity, 1952–1989. *Hemisphere*, *164*, 147–164.

Serreze, M. C., Carse, F., Barry, R. G., & Rogers, J. C. (1997). Icelandic low cyclone activity: Climatological features, linkages with the NAO, and relationships with recent changes in the Northern Hemisphere circulation. *Journal of Climate*, *10*(3), 453–464. https://doi.org/10.1175/1520-0442(1997)010%3C0453:ILCACF%3E2.0.CO;2

Shkolnik, I. M., & Efimov, S. V. (2013). Cyclonic activity in high latitudes as simulated by a regional atmospheric climate model: Added value and uncertainties. *Environmental Research Letters*, *8*(4), 45007. https://doi.org/10.1088/1748-9326/8/4/045007

Simmonds, I., Burke, C., & Keay, K. (2008). Arctic climate change as manifest in cyclone behavior. *Journal of Climate*, *21*(22), 5777–5796. https://doi.org/10.1175/2008JCLI2366.1

Simmonds, I., & Keay, K. (2009). Extraordinary September Arctic sea ice reductions and their relationships with storm behavior over 1979-2008. *Geophysical Research Letters*, *36*, L19715. https://doi.org/10.1029/2009GL039810

Simmonds, I., & Rudeva, I. (2012). The great arctic cyclone of August 2012. *Geophysical Research Letters*, *39*, L23709. https://doi.org/10.1029/2012GL054259

Simmonds, I., & Rudeva, I. (2014). A comparison of tracking methods for extreme cyclones in the Arctic basin. *Tellus A*, *66*(1), 1–13. https://doi.org/10.3402/tellusa.v66.25252

Skamarock, W. C., Klemp, J. B., Dudhia, J., Gill, D. O., Barker, D. M., Wang, W., & Powers, J. G. (2008). A description of the Advanced Research WRF Version 3. NCAR technical note, NCAR/TN-475+STR.

Smirnova, J., & Golubkin, P. (2017). Comparing polar lows in atmospheric reanalyses: Arctic system reanalysis versus ERA-Interim. *Monthly Weather Review*, *145*(6), 2375–2383. https://doi.org/10.1175/MWR-D-16-0333.1

Smith, B., Samuelsson, P., Wramneby, A., & Rummukainen, M. (2011). A model of the coupled dynamics of climate, vegetation and terrestrial ecosystem biogeochemistry for regional applications. *Tellus Series A: Dynamic Meteorology and Oceanography*, *63*(1), 87–106. https://doi.org/10.1111/j.1600-0870.2010.00477.x

Sommerfeld, A., Nikiema, O., Rinke, A., Dethloff, K., & Laprise, R. (2015). Arctic budget study of intermember variability using HIRHAM5 ensemble simulations. *Journal of Geophysical Research: Atmospheres*, *120*, 9390–9407. https://doi.org/10.1002/2015JD023153

Spengler, T., Claud, C., Heinemann, G., Spengler, T., Claud, C., & Heinemann, G. (2017). Polar low workshop summary. *Bulletin of the American Meteorological Society*, *98*(6), ES139–ES142. https://doi.org/10.1175/BAMS-D-16-0207.1

Takhsha, M., Nikiéma, O., Lucas-Picher, P., Laprise, R., Hernández-Díaz, L., & Winger, K. (2017). Dynamical downscaling with the fifth-generation Canadian regional climate model (CRCM5) over the CORDEX Arctic domain: Effect of large-scale spectral nudging and of empirical correction of sea-surface temperature. *Climate Dynamics*, 1–26. https://doi.org/10.1007/s00382-017-3912-6

Thompson, D. W. J., & Wallace, J. M. (1998). The Arctic oscillation signature in the wintertime geopotential height and temperature fields. *Geophysical Research Letters*, *25*(9), 1297–1300. https://doi.org/10.1029/98GL00950

Tilinina, N., Gulev, S. K., & Bromwich, D. H. (2014). New view of Arctic cyclone activity from the Arctic System Reanalysis. *Geophysical Research Letters*, *41*, 1766–1772. https://doi.org/10.1002/2013GL058924

Tsukernik, M., Kindig, D. N., & Serreze, M. C. (2007). Characteristics of winter cyclone activity in the northern North Atlantic: Insights from observations and regional modeling. *Journal of Geophysical Research*, *112*, D03101. https://doi.org/10.1029/2006JD007184

Ulbrich, U., Leckebusch, G. C., Grieger, J., Schuster, M., Akperov, M., Bardin, M. Y., et al. (2013). Are greenhouse gas signals of northern hemisphere winter extra-tropical cyclone activity dependent on the identification and tracking algorithm? *Meteorologische Zeitschrift*, *22*(1), 61–68. https://doi.org/10.1127/0941-2948/2013/0420

Vavrus, S. J. (2013). Extreme Arctic cyclones in CMIP5 historical simulations. *Geophysical Research Letters*, *40*, 6208–6212. https://doi.org/10.1002/2013GL058161

von Storch, H., Langenberg, H., & Feser, F. (2000). A spectral nudging technique for dynamical downscaling purposes. *Monthly Weather Review*, *128*(10), 3664–3673. https://doi.org/10.1175/1520-0493(2000)128%3C3664:ASNTFD%3E2.0.CO;2

Wang, X. L., Feng, Y., Chan, R., & Isaac, V. (2016). Inter-comparison of extra-tropical cyclone activity in nine reanalysis datasets. *Atmospheric Research*, *181*, 133–153. https://doi.org/10.1016/j.atmosres.2016.06.010

Wernli, H., & Schwierz, C. (2006). Surface cyclones in the ERA-40 da- taset (1958–2001). Part I: Novel identification method and global clima- tology. *Journal of the Atmospheric Sciences*, *63*(10), 2486–2507. https://doi.org/10.1175/JAS3766.1

Woollings, T., Hannachi, A., & Hoskins, B. (2010). Variability of the North Atlantic eddy-driven jet stream. *Quarterly Journal of the Royal Meteorological Society*, *136*(649), 856–868. https://doi.org/10.1002/qj.625

Zahn, M., & Von Storch, H. (2008). A long-term climatology of North Atlantic polar lows. *Geophysical Research Letters*, *35*, L22702. https://doi.org/10.1029/2008GL035769

Zahn, M., & von Storch, H. (2010). Decreased frequency of North Atlantic polar lows associated with future climate warming. *Nature*, *467*(7313), 309–312. https://doi.org/10.1038/nature09388

Zappa, G., Shaffrey, L. C., & Hodges, K. I. (2013). The ability of CMIP5 models to simulate North Atlantic extratropical cyclones. *Journal of Climate*, *26*(15), 5379–5396. https://doi.org/10.1175/JCLI-D-12-00501.1

Zhang, J., Lindsay, R., Schweiger, A., & Steele, M. (2013). The impact of an intense summer cyclone on 2012 Arctic sea ice retreat. *Geophysical Research Letters*, *40*, 720–726. https://doi.org/10.1002/grl.50190

Zhang, J., & Rothrock, D. A. (2003). Modeling global sea ice with a thickness and enthalpy distribution model in generalized curvilinear coordinates. *Monthly Weather Review*, *131*(5), 845–861. https://doi.org/10.1175/1520-0493(2003)131h0845:MGSIWAi2.0.CO;2

Zhang, W., Jansson, C., Miller, P. A., Smith, B., & Samuelsson, P. (2014). Biogeophysical feedbacks enhance the Arctic terrestrial carbon sink in regional Earth system dynamics. *Biogeosciences*, *11*(19), 5503–5519. https://doi.org/10.5194/bg-11-5503-2014

Zhang, X., Walsh, J. E., Zhang, J., Bhatt, U. S., & Ikeda, M. (2004). Climatology and interannual variability of Arctic cyclone activity: 1948-2002. *Journal of Climate*, *17*(12), 2300–2317. https://doi.org/10.1175/1520-0442(2004)017%3C2300:CAIVOA%3E2.0.CO;2

Erratum

In the originally published version of this article, a portion of Figure 4 was left out. This information has since been added to the figure, and this version may be considered the authoritative version of record.